Crystal Structure of 4H BaRuO₃ : High Pressure Phase Prepared at Ambient Pressure

Seung-Tae Hong and Arthur W. Sleight[1]

Department of Chemistry, Oregon State University, Corvallis, Oregon 97331-4003

Single crystals of $BaRuO_3$ were grown using a $BaCl_2$ flux at ambient pressure. Most of the crystals had the nine-layer rhombohedral structure (9R) which is considered to be the stable form of $BaRuO_3$ at ambient pressure. However, some $BaRuO_3$ crystals in this preparation had the four-layer hexagonal (4H) structure which had been considered as a phase produced only at high pressure (15–30 kbar). The crystal structure of 4H $BaRuO_3$ was refined for the first time. Single crystal X-ray diffraction data gave a space group of $P6_3/mmc$ (No. 194), $a = 5.729(1)$ Å, $c = 9.500(1)$ Å, $Z = 4$, a final conventional R (based on F_0) of 2.01%, and a $wR2$ (based on F_0^2) of 4.07%. The structure of 4H $BaRuO_3$ may be described as perovskite-related with a four-layer stacking of BaO_3 layers in the sequence $hchc$. This leads to pairs of face-sharing RuO_6 octahedra which are connected to other octahedra by corner sharing. The Ru–Ru distance in the Ru_2O_9 dimer of 4H $BaRuO_3$ is 2.537(1) Å which indicates the presence of a metal–metal bond. © 1997 Academic Press

INTRODUCTION

Only a few crystal structures of compounds in the Ba–Ru–O ternary system have been reported. The most well known and well characterized compound is $BaRuO_3$ (1, 2). The X-ray patterns of Ba_3RuO_6 (3, 4) and Ba_4RuO_5 (5) were reported, but recently they were found to be the same compound with the actual formula $Ba_5Ru_2O_{10}$ (6). The chemical formula of Ba_2RuO_4 (4) reportedly prepared at atmospheric pressure was also found to be incorrect: the actual formula is $Ba_5Ru_3O_{12}$ (7). When Ba_2RuO_4 is prepared at high pressure, it has the K_2NiF_4 structure (8). The compounds $BaRu_4O_9$ and Ba_9RuO_{11} are also reported in the literature but without any information on their crystal structures (4, 5). The other known compounds in the Ba–Ru–O system are $Ba_4Ru_3O_{10}$ (7) and $BaRu_6O_{12}$ (9).

Perovskite-related compounds ABO_3 can be described based on the stacking of compact hexagonal AO_3 layers with small cations, B, occupying octahedral holes between the layers (10). The close-packed AO_3 layers tend to change their stacking sequence from cubic to hexagonal depending on the size of metal ions, chemical bonding nature, and synthetic conditions. If the stacking is entirely cubic, in a sequence of *abc*, the BO_6 octahedra share only corners leading to a cubic or more often a pseudo-cubic perovskite (3C) structure. If all of the layers are hexagonal close packed in a sequence *ab*, however, the BO_6 octahedra share faces to form chains along the *c* axis, as observed in 2H $BaNiO_3$ (11). In between the two extreme cases, there are several intermediate structures corresponding to different percentages of cubic stacking (corner-shared octahedra) and hexagonal stacking (face-shared octahedra). There is a well known tendency for these ABO_3 compounds to transform to structures containing more cubic packing and fewer face-shared octahedra as the synthesis pressure is increased (12). A typical example is $BaRuO_3$ which shows several different structures as a function of pressure (Fig. 1) (12, 13). At atmospheric pressure, $BaRuO_3$ has the 9R polytype structure with a *hhchhchhc* stacking sequence (2) (Fig. 1a). This structure transforms at 15 kbar to the 4H structure (*hchc*) (Fig. 1b) and further transforms to the 6H structure (*cchcch*) (Fig. 1c) at 30 kbar. A study of the $BaRuO_3$–$SrRuO_3$ phase diagram as a function of pressure indicated that $BaRuO_3$ would have the perovskite structure (Fig. 1d) of $SrRuO_3$ at about 120 kbar (12).

EXPERIMENTAL

Synthesis

Single crystals of $BaRuO_3$ were prepared during attempts to prepare new compounds in the Ba/Ru/W/O system. Reactants were high purity $BaCO_3$, RuO_2, and WO_3. These reactants were mixed in a 6:2:2 Ba:Ru:W ratio, pressed into a pellet, heated at 1120°C for 12 h, heated again at 1120°C for 17 h, and finally at 1200°C for 54 h with intermediate grindings and pressings. This product was then mixed with a tenfold excess of $BaCl_2$, heated to 1200°C for 10 h, and cooled slowly to room temperature. Black crystals formed together with thin orange barium ruthenium
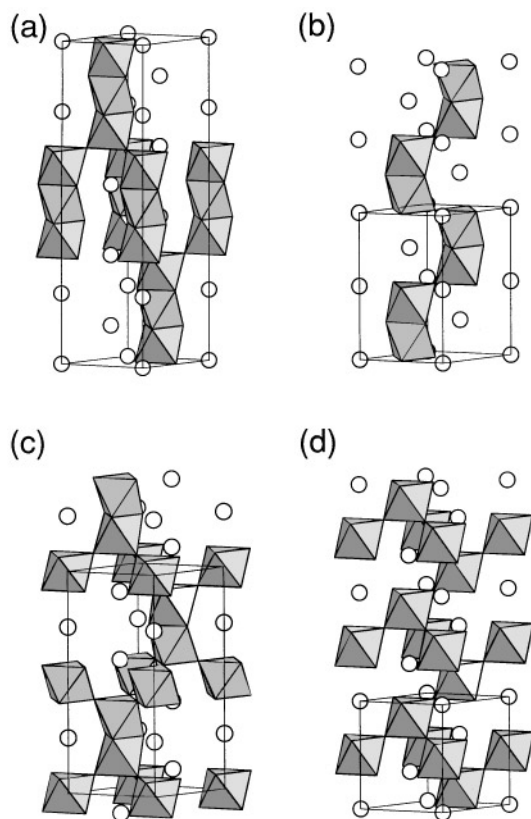
FIG. 1. The various polytypes of BaRuO$_3$: (a) 9R, (b) 4H, (c) 6H and (d) 3C. The network of RuO$_6$ octahedra are shown. The circles represent Ba cations. The unit cells are also shown.

TABLE 1
Crystallographic Parameters for 4H BaRuO$_3$

Formula	BaRuO$_3$
fw	286.41
Crystal size, mm	$0.14 \times 0.17 \times 0.10$
Color	black
a, Å	5.729(1)
c, Å	9.500(1)
V, Å^3	270.03(7)
μ (MoKα), mm^{-1}	19.831
Radiation	MoKα ($\lambda = 0.71073$ Å)
	Graphite monochromated
ρ_{calc}, g/cm^3	7.045
Space group	$P6_3/mmc$, No.194
Z	4
Diffractometer	Rigaku AFC6R
T, K	296
Octants measured	$h, k, \pm l$
Scan mode	ω–2θ
$2\theta_{max}$	60
No. of reflection measured	620
No. of unique data, R_{int}	176, 0.033
No. of observed refined [$F_0 > 4\sigma(F_0)$]	161
No. of parameters refined	17
Refined method	full-matrix least squares on $|F|^2$
$F_0(000)$	496
$R1$ [$I > 2\ \sigma(I)$]^a, $R1^a$ (all data)	0.0201, 0.0240
$wR2$ [$I > 2\ \sigma(I)$]^a, $wR2^a$ (all data)	0.0407, 0.0432
Goodness of fit [$I > 2\ \sigma(I)$]	1.270
$(\Delta\rho)_{max}$, $(\Delta\rho)_{min}$, e/Å^3	0.81, -0.87
Extinction method	SHELXL
Extinction coeff.	$3.8(2) \times 10^{-2}$

$^a R1 = ||F_0| - |F_c||/\sum|F_0|$ and $wR2 = \sqrt{(w(F_0^2 - F_c^2)^2/\sum wF_0^4)}$, $w = 1/[\sigma^2(F_0^2) + (0.002P)^2 + 0.3069P]$, where $P = (\max(F_0^2, 0) + 2F_c^2)/3$.

tungstate plate-like crystals which were separated from BaCl$_2$ by leaching with dilute HCl. Most of the black crystals were 9R BaRuO$_3$; however, a few were found from Laue and precession photographs to be 4H BaRuO$_3$. Several crystals were analyzed by electron microprobe. No W or Cl was found, and the Ba:Ru ratio was one.

Single Crystal Structural Determination

Single crystals were first examined by the Laue and precession techniques to establish cell parameters, symmetry, and suitability for intensity data collection. These techniques established a Laue symmetry group of 6/*mmm*. Intensity data for a 4H BaRuO$_3$ crystal were collected at room temperature using a Rigaku AFC6R diffractometer with graphite monochromated MoKα radiation. The diffraction data were corrected for Lorentz and polarization effects and for absorption using the average of ψ scans of three reflections at different θ values. Details of the data collection and refinement are given in Table 1. The hexagonal unit cell parameters were refined to $a = 5.729(1)$ Å and $c = 9.500(1)$ Å from 20 reflections with 2θ values from 30° to 35°. An examination of the data collected confirmed the 6/*mmm*

Laue class and showed that the condition for the observed reflections is $hh2\bar{h}l$, $l = 2n$. The possible space groups are thus $P6_3/mmc$, $P6_3mc$, or $P\bar{6}2c$. The structure was determined by the interpretation of Patterson maps in all three space groups using SHELXS-86 (14), which suggested positions for the barium and ruthenium atoms. The positions of the oxygen atoms were progressively located from Fourier difference maps during the course of the refinement (program SHELXL93) (15). The best refinement (stable convergence, lowest residuals) was obtained in space group $P6_3/mmc$ (No. 194). The final conventional R (based on F_0) and wR (based on F_0^2), including a weighting scheme and anisotropic thermal motions for all atoms, decreased to $R = 2.01\%$ and $wR2 = 4.08\%$ for 161 independent reflections with F_0 greater than $4\sigma(F_0)$.

RESULTS AND DISCUSSION

The positional parameters and thermal parameters for 4H BaRuO$_3$ are given in Table 2, and the main interatomic distances and angles appear in Table 3. The crystal structure

TABLE 2
Atomic Coordinates and Isotropic Thermal Parameters
($\text{Å}^2 \times 10^3$) for 4H BaRuO$_3$

Atom	Site	x	y	z	$U_{eq}{}^a$
Ba(1)	2a	0	0	0	11.4(3)
Ba(2)	2c	1/3	2/3	1/4	8.2(2)
Ru	4f	2/3	1/3	0.11647(6)	6.1(2)
O(1)	6g	1/2	1/2	0	10 (1)
O(2)	6h	0.354(1)	0.1772(6)	1/4	8.6(9)

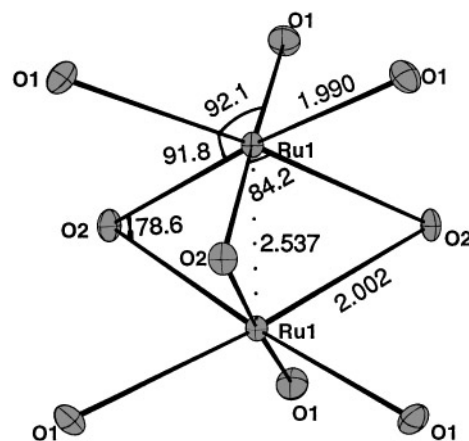|	U_{11}	U_{22}	U_{33}	U_{23}	U_{13}	U_{12}
Ba(1)	8.1(3)	U_{11}	18.1(4)	0	0	4.03(15)
Ba(2)	7.7(3)	U_{11}	9.2(4)	0	0	3.83(15)
Ru	5.5(3)	U_{11}	7.3(4)	0	0	2.75(14)
O(1)	11(2)	U_{11}	U_{11}	1.9(8)	$-U_{23}$	6 (2)
O(2)	4(2)	8(2)	12(2)	0	0	0.5 U_{11}

^{a} Equivalent U_{iso} defined as one-third of the trace of the orthogonalized U_{ij} tensor.

of 4H BaRuO$_3$ is shown schematically in Fig. 1b and in detail in Fig. 2. The structure of 4H BaRuO$_3$ may be described as a perovskite-related compound with a four-layer stacking of BaO$_3$ layers in the sequence of *hchc*. This leads to pairs of face-sharing octahedra, and these pairs are connected by corner sharing of the octahedra. Such a four-layer hexagonal (4H) structure is also found for some other perovskite-related compounds such as Ba$_{1-x}$Sr$_x$RuO$_3$ ($0.1 < x < 0.3$) (12, 16), SrMnO$_3$ (17–19), BaRu$_{0.9}$Fe$_{0.1}$O$_3$ (20), BaMnO$_3$ (17, 21, 22), BaCrO$_3$ (23), and BaRhO$_3$ (24), the last three compounds being prepared at high pressure. The average Ru–O distance in 4H BaRuO$_3$, 1.996 Å, is close to those reported for tetravalent ruthenium compounds as in 9R BaRuO$_3$ (1.994 Å) (2), Ba$_4$ZrRu$_3$O$_{12}$ (2.001 Å) (25), and Ba$_3$TiRu$_2$O$_9$ (1.998 Å) (26).

The Ru$_2$O$_9$ dimer in 4H BaRuO$_3$ (Fig. 2) is typical of many ruthenium compounds such as Ba$_3$Ru$_2$MO$_9$ (M = Ti,

FIG. 2. Local structure of the dimeric unit [Ru$_2$O$_9$]. Thermal ellipsoids are used for atoms. Some bond distances (Å) and bond angles (degree) are shown.

Fe, Co, Ni, Cu, Zn, Cd, In, Bi, Mg, Ca, Sr) (26–32), Ba$_2$RuBiO$_6$ (33), Ba$_5$Ru$_2$O$_{10}$ (6), Sr$_4$Ru$_2$O$_9$ (34), Ba$_5$Ru$_2$O$_9$Cl$_2$ (35), and Ba$_4$Ru$_3$MO$_{12}$ (M = Li, Na) (36). Examples showing a Ru$_3$O$_{12}$ ruthenium trimer are 9R BaRuO$_3$ (Fig. 1a), Ba$_4$Ru$_3$MO$_{12}$ (M = Nb, Ta) (37), Ba$_4$ZrRu$_3$O$_{12}$ (25), Ba$_4$Ru$_3$O$_{10}$ (7), and Ba$_5$Ru$_3$O$_{12}$ (7). The common occurrence of dimers and trimers suggests that ruthenium has a preference for face-shared octahedra. Concerning the dimer units Ru$_2$O$_9$ in 4H BaRuO$_3$, the Ru–Ru distance (2.537 Å) is smaller than the Ru–Ru distance in the metal itself (2.65 Å) and close to that found in tetravalent ruthenium compounds such as 9R BaRuO$_3$ (2.55 Å) (2), Ba$_4$ZrRu$_3$O$_{12}$ (2.529(6) Å) (25), Ba$_3$TiRu$_2$O$_9$ (2.515 Å) (26), and Ba$_4$Ru$_3$O$_{10}$ (2.568 Å) (7), which is also comparable with the value in La$_4$Ru$_6$O$_{19}$ (2.488 Å) (38). It is also smaller than the metal–metal distances in the isostructural 4H compounds as in BaMnO$_3$ (2.62 Å) (21), BaCrO$_3$ (2.611 Å) (23), and BaRhO$_3$ (2.628 Å) (24). If the ruthenium atoms were exactly midway between BaO$_3$ layers, forming ideal octahedra, then the Ru–Ru distance in 4H BaRuO$_3$ would be 2.375 Å. This is significantly smaller than the observed value (2.537 Å), indicating the existence of some repulsion between the Ru metal ions. This results in a distorted octahedron with O2–O2 distances being shorter than O1–O1 or O1–O2 distances (Table 2 and Fig. 2).

Some Ru–Ru distances in oxides are given vs ruthenium oxidation state in Fig. 3. All are for octahedra sharing faces except La$_4$Ru$_6$O$_{19}$ where the octahedra share edges in pairs. The electronic configurations for Ru(IV) and Ru(V) are low-spin d^4 and d^3, respectively. There are therefore more unpaired electrons available for metal–metal bonding for Ru(V) than for Ru(IV). The longer Ru–Ru distance for the Ru(V) compounds indicates then that the metal–metal bond no longer exists, despite the more favorable electronic configuration. The Ru–Ru distance in the Ru(V) compounds is

TABLE 3
Selected Bond Distances (Å) and Angles (deg) for 4H BaRuO$_3$

Ba(1)–O(1) × 6	2.8645(5)	Ru–Ru	2.537(1)
Ba(1)–O(2) × 6	2.955(3)	Ru–Ba(1) × 3	3.4878(6) × 3
Ba(2)–O(2) × 6	2.8664(6)	Ru–Ba(2) × 3	3.4816(7) × 3
Ba(2)–O(1) × 6	2.8941(3)	Ru–Ba(2′) × 1	3.5425(6) × 1
Ru–O(1) × 3	1.9898(4)	O(1)–Ru–O(1)	92.07(2) × 3
Ru–O(2) × 3	2.002(4)	O(1)–Ru–O(2)	91.76(7) × 6
		O(1)–Ru–O(2)	174.5(1) × 3
O1–O1 × 3	2.8645(5)	O(2)–Ru–O(2)	84.2(2) × 3
O1–O2 × 3	2.8660(14)	Ru–O(1)–Ru	180
O2–O2 × 3	2.684(9)	Ru–O(2)–Ru	78.6(2)
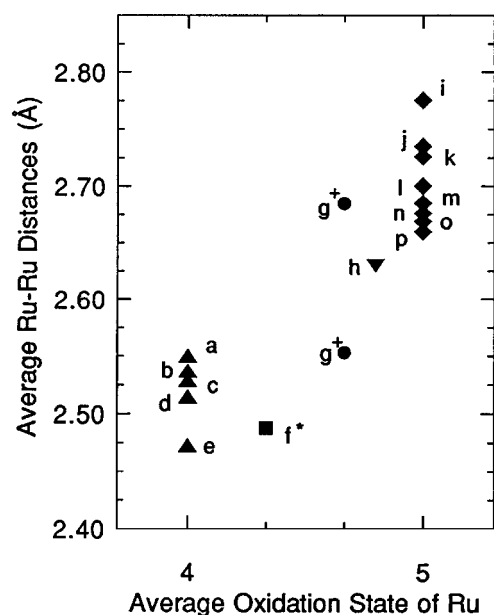
FIG. 3. Average oxidation state of Ru vs average Ru–Ru distances in face-sharing dimeric units [Ru_2O_9] in various Ru compounds; (a) 9R $BaRuO_3$ (2), (b) 4H $BaRuO_3$ (this work), (c) $Ba_4ZrRu_3O_{12}$ (25), (d) $Ba_3TiRu_2O_9$ (26), (e) $Ba_{5/6}Sr_{1/6}RuO_3$ (16), (f) $La_4Ru_6O_{19}$ (38), (g) $Ba_5(Ir,Ru)_3O_{12}$ (40), (h) $Ba_6Ru_{2.5}Mn_{0.5}O_{12}Cl_2$ (41), (i) $Sr_4Ru_2O_9$ (34), (j) $Ba_5Ru_2O_{10}$ (6), (k) $Ba_5Ru_2O_9Cl_2$ (35), (l) $Ba_4Ru_3LiO_{12}$ (36), (m) $Ba_3Ru_2MO_9$ (M = Zn, Ni) (42) at 5 K, (n) $Ba_3Ru_2MO_9$ (M = Co, Sr) (43, 42), (o) $Ba_3MgRu_2O_9$ (31), and (p) $Ba_4Ru_3NaO_{12}$ (36). (∗) Edge-shared Ru–Ru; (+) Two distinct distances in one structure.

now similar to the Ti–Ti distance (2.69 Å) (39) across the shared octahedral face in hexagonal $BaTiO_3$ where a metal–metal bond is not possible due to the d^0 configuration of Ti(IV). Two factors may combine to prevent metal–metal bond formation with Ru(V) compounds. There will be some increased repulsion between Ru cations due to the increase in cation charge. Also, the d orbital contraction which occurs on going from Ru(IV) to Ru(V) decreases the d–d orbital overlap and will therefore destabilize a metal–metal bond.

Our finding of 4H $BaRuO_3$ crystals mixed with 9R $BaRuO_3$ crystals in an ambient pressure preparation might be considered surprising because 4H $BaRuO_3$ is reported to be formed only above a pressure of 15 kbar. However in the $BaMnO_3$ system (17), both 9R and 4H $BaMnO_3$ were found in the same high pressure preparation. Our precession photographs of the $BaRuO_3$ crystals sometimes showed both 9R and 4H $BaRuO_3$ to be present and aligned in such a way as to suggest that a small crystal of 9R $BaRuO_3$ had grown epitaxially on the 001 surface of a 4H $BaRuO_3$ crystal. Despite the fact that electron microprobe analysis showed no evidence for W in our 4H $BaRuO_3$ crystals, there is the possibility that the W present during our synthesis served somehow to catalyze or nucleate the 4H $BaRuO_3$ structure outside of its normal stability range.

REFERENCES

1. J. J. Randall and R. Ward, *J. Am. Chem. Soc.* **81,** 2629 (1959).
2. P. C. Donohue, L. Katz, and R. Ward, *Inorg. Chem.* **4,** 306 (1965).
3. I. I. Prosychev and I. S. Sharplygin, *Russ. J. Inorg. Chem.* **25,** 489 (1980).
4. T. L. Popova, N. G. Kisel, V. I. Krivobok, and V. P. Karlov, *Sov. Prog. Chem.* **48,** 8 (1983).
5. M. I. Gadzhiev and I. S. Shaplygin, *Russ. J. Inorg. Chem.* **29,** 1230 (1984).
6. C. Dussarrat, J. Fompeyrine, and J. Darriet, *Eur. J. Solid State Inorg. Chem.* **31,** 289 (1994).
7. C. Dussarrat, F. Grasset, R. Bontchev, and J. Darriet, *J. Alloys Comp.* **233,** 15 (1996).
8. J. A. Kafalas and J. M. Longo, *J. Solid State Chem.* **4,** 55 (1972).
9. C. C. Torardi, *Mater. Res. Bull.* **20,** 705 (1985).
10. L. Katz and R. Ward, *Inorg. Chem.* **3,** 205 (1964).
11. J. J. Lander, *Acta Crystallogr.* **4,** 148 (1951).
12. J. M. Longo and J. A. Kafalas, *Mater. Res. Bull.* **3,** 687 (1968).
13. J. B. Goodenough, J. A. Kafalas, and J. M. Honig, in "Preparative Methods in Solid State Chemistry" (P. Hagenmuller, Ed.), pp. 1–69. Academic Press, New York, 1972.
14. G. M. Sheldrick, "SHELXS-86 User Guide," Crystallography Department, University of Göttingen, Germany, 1986.
15. G. M. Sheldrick, "SHELXL93, A Program for Refinement of Crystal Structures," University of Göttingen, Germany, 1993.
16. P. C. Donohue, L. Katz, and R. Ward, *Inorg. Chem.* **5,** 335 (1966).
17. B. L. Chamberland, A. W. Sleight, and J. F. Weiher, *J. Solid State Chem.* **1,** 506 (1970).
18. Y. Syono, S. Akimoto, and K. Kohn, *J. Phys. Soc. Jpn.* **26,** 993 (1969).
19. T. Negas and R. S. Roth, *J. Solid State Chem.* **1,** 409 (1970).
20. S. Kemmler-Sack and A. Ehmann, *J. Solid State Chem.* **44,** 366 (1982).
21. A. Hardy, *Acta Crystallogr.* **15,** 179 (1962).
22. T. Negas and R. S. Roth, *J. Solid State Chem.* **3,** 323 (1971).
23. B. L. Chamberland, *J. Solid State Chem.* **43,** 309 (1982).
24. B. L. Chamberland and J. B. Anderson, *J. Solid State Chem.* **39,** 114 (1981).
25. C. H. De Vreugd, H. W. Zandbergen, and D. J. W. Ijdo, *Acta Crystallogr.* **C 40,** 1987 (1984).
26. D. Verdoes, H. W. Zandbergen, and D. J. W. Ijdo, *Acta Crystallogr.* **C 41,** 170 (1985).
27. P. C. Donohue, L. Katz, and R. Ward, *Inorg. Chem.* **5,** 339 (1966).
28. I. Fernandez, R. Greatrex, and N. N. Greenwood, *J. Solid State Chem.* **34,** 121 (1980).
29. J. Darriet, M. Drillon, G. Villeneuve, and P. Hagenmuller, *J. Solid State Chem.* **19,** 213 (1976).
30. von H.-U. Schaller, and S. Kemmler-Sack, *Z. Anorg. Allg. Chem.* **473,** 178 (1981).
31. U. Treiber, U. Kemmler-Sack, and A. Ehmann, *Z. Anorg. Allg. Chem.* **487,** 189 (1982).
32. J. Darriet, R. Bontchev, C. Dussarrat, F. Weill, and B. Darriet, *Eur. J. Solid State Inorg. Chem.* **30,** 273 (1993).
33. J. Darriet, R. Bontchev, C. Dussarrat, F. Weill, and B. Darriet, *Eur. J. Solid State Inorg. Chem.* **30,** 287 (1993).
34. C. Dussarrat, J. Fompeyrine, and J. Darriet, *Eur. J. Solid State Inorg. Chem.* **32,** 3 (1995).
35. Ch. Lang and Hk. Müller-Buschbaum, *Z. Anorg. Allg. Chem.* **587,** 39 (1990).

36. P. D. Battle, S. H. Kim, and A. V. Powell, *J. Solid State Chem.* **101,** 161 (1992).

37. R. Greatrex and N. N. Greenwood, *J. Solid State Chem.* **31,** 281 (1980).

38. F. Abraham, J. Trehoux, and D. Thomas, *Mater. Res. Bull.* **12,** 43 (1977).

39. J. Akimoto, Y. Gotoh, and Y. Oosawa, *Acta Crystallogr.* **C 50,** 160 (1994).

40. Ch. Lang and Hk. Müller-Buschbaum, *Z. Anorg. Allg. Chem.* **580,** 71 (1990).

41. M. Neubacher and Hk. Müller-Buschbaum, *Z. Anorg. Allg. Chem.* **602,** 143 (1991).

42. P. Lightfoot and P. D. Battle, *J. Solid State Chem.* **89,** 174 (1990).

43. H. W. Zandbergen and D. J. W. Ijdo, *Acta Crystallogr. C* **40,** 919 (1984).